

Correlated three-electron continuum states in triple ionization by fast heavy-ion impactM. Schulz,^{1,2} R. Moshhammer,¹ W. Schmitt,¹ H. Kollmus,¹ R. Mann,³ S. Hagmann,⁴ R. E. Olson,² and J. Ullrich¹¹*Universität Freiburg, Fakultät für Physik, D-79104 Freiburg, Germany*²*Department of Physics, University of Missouri–Rolla, Rolla, Missouri 65409*³*Gesellschaft für Schwerionenforschung, D-64291 Darmstadt, Germany*⁴*Department of Physics, Kansas State University, Manhattan, Kansas 66506-2601*

(Received 6 July 1999; published 5 January 2000)

We have performed a kinematically complete experiment for triple ionization in atomic collisions. Data were obtained for 3.6-MeV/amu Au⁵³⁺ impact on Ne. A specific Dalitz representation was developed allowing one to plot in a single spectrum the energy of all three ionized electrons and, simultaneously, obtain information on their emission angles with respect to the projectile direction. The data show distinct fragmentation patterns favoring very asymmetric energy partitionings with one fast and two slow electrons. They are compared to various Classical Trajectory Monte Carlo (CTMC) models. The experimental results are well described only if the electron-electron interaction is included throughout the collision and surprisingly, if the classically modeled electrons are fully correlated in the initial state.

PACS number(s): 34.10.+x, 34.50.Fa

I. INTRODUCTION

One of the fundamental, unsolved problems in physics is the quantitative description of time-dependent many-body systems. In various areas, like e.g., atomic, molecular, nuclear, and particle physics, the same basic question is often the focus of experimental and theoretical research: what is the time evolution of a system of mutually interacting particles? Both the classical equations of motion and the Schrödinger equation are not solvable in closed form for more than two interacting particles. In atomic physics where the long range Coulomb potential is involved, one is faced with the additional problem that it is extremely difficult to find appropriate numerical methods. As a result, even the most simple and basic atomic many-body systems, involving only 3 or 4 particles, are not fully understood.

For ionization the situation is particularly complicated since continuum states of several particles are involved. In general, the ionized electrons depart from both the recoiling target ion and the projectile ion to infinite distances. However, because of the long range nature of the Coulomb force, the electrons still interact with both heavy particles and with each other at all distances. Thus, the transition amplitudes in principle involve an integration over infinite space. In contrast, for excitation or capture reactions the electrons remain with one of the collision partners and the integration can to a good approximation be limited to finite space. Similarly, the integration can often be reduced to finite space if a short range interaction potential is involved, like in nuclear physics. Because of the long range nature of the Coulomb potential ionization processes belong to the most delicate time-dependent reactions to describe theoretically.

The complexity of ionization processes is also reflected by the fact that in spite of tremendous efforts and significant progress over the last two decades, the agreement between theory and experimental data is often not satisfactory. Especially at low projectile velocities, theory has great difficulty in achieving good agreement with experiment even for single ionization in the most simple ion-atom collision systems like protons impinging on hydrogen or helium [1–3]. For double

ionization, our understanding is even less complete. Few attempts have been made to treat double ionization by fast charged particles [4–8] and not a single quantum mechanical approach has been made to calculate differential multiple ionization cross sections for any type of projectile. Total multiple ionization cross sections have been calculated only recently beyond an independent electron model using time-dependent density functional methods [9].

Given these theoretical problems with ionization processes, it is critically important to obtain experimental data as detailed as possible. Whereas kinematically complete experiments on single ionization have been feasible for more than two decades for fast electron impact [10,11] such measurements for ion impact succeeded only recently [12]. For both projectile species experiments are in good agreement with results from increasingly sophisticated theoretical models both in the perturbative and nonperturbative regime. This leads to a sound, though not complete understanding of single ionization in fast collisions. As mentioned above, at low velocities, however, basic difficulties remain.

Kinematically complete experiments on double ionization of helium by charged particles became available in 1996 for heavy ions in the non-perturbative regime [13]. During the last year first experiments in the perturbative regime were reported for electron [14,15] as well as fast ion impact [16]. In the perturbative regime comparison of the experimental data with various model calculations including the final state interaction as well as the initial state correlation on different levels of sophistication has led to two important conclusions: first, the calculated results sensitively depend on the specific correlated initial state wave functions used. For fast heavy ion impact (with comparable kinematics and perturbation as in the present study) it was found that the two electrons are emitted essentially simultaneously (within attoseconds) with a relatively small momentum transfer from the projectile [13]. This revitalized the early hope that the measured correlated final state electron momenta represent instantaneous images (“snap shots”) of the correlated initial state. Second, the effect of the final state interaction was found to depend on the specific correlated initial wavefunc-

tion as well. Thus, it was concluded that an independent discussion of the contributions of the electron-electron interaction in the initial and final state, respectively, is problematic. They mutually depend on each other and their effect cannot be separated.

In this paper we report on correlated momenta of three electrons in the continuum after triple ionization of neon in collisions with 3.6 MeV/amu Au⁵³⁺ ions. It is the second in a series of three papers where we approach the dynamic many-electron problem. We realize that an accurate theoretical treatment of transitions of more than two electrons from bound to continuum states appear to be beyond computational capacities in the near future. This makes experimental information all the more important.

Four basic questions are addressed by our studies. First, which features of many-electron processes, i.e., which of the observables, can be described within an independent electron model (IEM)? How do the effective single-particle states need to be constructed and what are the limitations of such an approach? In our first paper we focused on this question by analyzing the differential projectile energy-loss spectra for different degrees of ionization [17]. This is a rather global parameter since it is essentially determined by the sum energy of all ejected electrons, but it is nevertheless important for numerous applications (e.g., stopping powers of dense matter, plasma physics, tumor therapy by heavy ion irradiation). It was demonstrated that the energy-loss spectra can be described almost perfectly in an independent electron picture. They could be reproduced for Q -fold ionization ($Q = 2+$ to $6+$) by a convolution procedure if only the energy spectrum of a single electron randomly picked out of the Q electrons was measured. Furthermore, the energy-loss spectra were well described by n -body classical trajectory Monte Carlo (nCTMC) calculations where the electron-electron interaction is considered only in terms of a screening of the target nucleus.

The second question, to be addressed in this paper, concerns signatures and relative importance of possible correlations between the fragments of the collision, i.e., properties which go beyond an IEM. Do certain observables of one electron depend in a characteristic way on those of the others and, if so, what are these observables? Since no such effects were observed in the sum energy of all ionized electrons, here we put emphasis on the analysis of the distribution of the continuum energy and momentum of the three individual electrons in triple ionization. Indeed, distinct fragmentation patterns are found showing the limitations of an independent particle description. nCTMC calculations, which were successfully applied in the previous paper to calculate the total energy transferred to all ionized electrons, cannot account for the observed patterns. In a series of model calculations we try to investigate the origin of the structures. Surprisingly, strong correlations between the electrons in the initial state as well as the electron-electron interaction throughout the collision are needed to achieve reasonable qualitative agreement with the data.

The third question, also to be addressed in this paper, deals with the details of the transition dynamics from a many-electron bound state to a continuum state. A stationary

target atom is an entity with a high degree of order enforced by the Pauli exclusion principle combined with quantization rules. If a many-electron atom would follow the rules of classical mechanics, in contrast, the electrons would behave much more chaotically due to their mutual Coulomb repulsion. The question is, to what extent does the final continuum state reflect the ordered structure of the initial state and to what extent does the final state Coulomb interaction in the continuum imposes a new ordered structure unrelated to the initial state?

The fourth question is related to the previous question, but also reaches far into the future: is it possible to find a transition in the theoretical treatment from a few particle description incorporating all mutual interactions to a more global, statistical or thermodynamical approach. For one or two particles, the problem is exactly solvable if the interaction potential is known. For a very large number of constituents, statistical approaches work very well. Thus, these two extreme situations can be considered as understood or at least sophisticated theoretical models are available. In between we are faced with a dark zone where theoretical concepts are missing. Future experiments at the GSI storage ring will provide the unique opportunity to access the complete kinematics of double to potentially ten-fold ionization. Such experiments deliver maximum amount of information on systems with an intermediate number of constituents where, in addition, the pairwise two-body interaction potentials are precisely known.

II. EXPERIMENT

The final state of an ion-atom collision system after triple ionization involves 5 unbound particles (3 electrons, the projectile, and the recoiling target ion). Thus, a kinematically complete experiment requires to measure the momentum vectors of 4 particles. The fifth momentum vector can then be deduced from momentum conservation. In the experiment described below, the momentum vectors of the 3 ionized electrons and the recoil ion were measured.

The experiment was performed at the Gesellschaft für Schwerionenforschung (GSI) in Darmstadt. A 3.6 MeV/amu Au⁵³⁺ beam was delivered by the Universal Linear Accelerator (UNILAC) and collimated to a size of about $1 \times 1 \text{ mm}^2$. The projectile beam was then crossed with an atomic Ne beam from a supersonic gas jet. A switching magnet was used to analyze the projectile charge state after the collision and the projectiles which did not change charge state were detected by a scintillator.

The three stage supersonic gas jet is required to cool the target gas in order to minimize the momentum spread of the recoil ions due to their thermal motion. The first stage is a reservoir containing Ne gas at a pressure of about 8 atm. Some of the gas can escape this reservoir through a $30 \mu\text{m}$ nozzle into the second stage, which is kept at a vacuum of 10 mTorr by a roots pump. The large pressure gradient between the first two stages leads to adiabatic expansion of the gas, which results in a cooling of the gas in the direction of the gradient to a temperature of less than 1 K. In the plane perpendicular to the pressure gradient, the gas is cooled by a

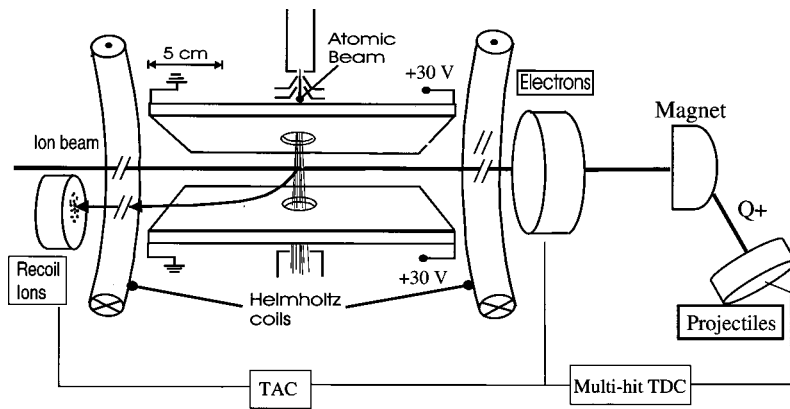


FIG. 1. Schematic picture of the recoil-ion and electron momentum spectrometer. The multi-hit time to digital converter (TDC) allows us to detect up to three electrons for each collision event simultaneously.

skimmer with a diameter of $300\ \mu\text{m}$, which collimates those Ne atoms out which have a non-zero momentum component in that plane. In the third stage, which is separated from the second stage by the skimmer, a vacuum of 10^{-5} Torr is maintained by a 400 l/s turbomolecular pump. A second skimmer with a diameter of $600\ \mu\text{m}$ separates the collision chamber from the third stage of the jet. At the intersection point with the projectile beam the gas jet has a diameter of about 1 mm and a thickness of $10^{11}/\text{cm}^2$. With the full gas load in the reservoir of the gas jet, the vacuum in the collision chamber was 10^{-7} Torr.

The electrons and recoil ions were momentum-analyzed by the same spectrometer system, which is shown in Fig. 1. It consists of two parallel resistive plates 22 cm in length and separated by a distance of 7 cm which are oriented along the projectile beam axis. An electric field was generated by applying a voltage of 30 V across the plates so that the electrons were extracted parallel and the recoil ions antiparallel to the projectile beam direction. After traversing a 22 cm long field free drift tube following the extraction region, the recoil ions and electrons were detected by two two-dimensional channel plate detectors with diameters of 50 and 80 mm, respectively.

The extraction field was not strong enough to guide a sufficiently large fraction of the electrons onto the detector. Therefore, a uniform magnetic field of 20 G in the same direction as the electric extraction field was generated by two Helmholtz coils. As a result, the electrons were forced into cyclotron motion with a radius proportional to the transverse momentum component of the electrons. For transverse momenta of less than 3.5 a.u. the cyclotron radius was small enough for the electrons to hit the detector.

One of the most challenging aspects of this experiment was to simultaneously record the time of flight and position information of three electrons emitted in the same collision event and hitting the same detector. This was accomplished by using a delay line anode in conjunction with a multi-hit time to digital converter (TDC). Two wires were wrapped around the anode in the x - and y -direction. For each electron one timing signal was recorded from the channel plate and two timing signals from the ends of each wire. The propagation times of the signal through the wire from the point where the electron hit the anode to both ends of the wire are proportional to the distance of that point to the corresponding end. Therefore, the position information for each direction is

given by the time difference between the signals at the two ends of each wire. The multi-hit TDC allowed us to record the same signals for further electrons hitting the detector with some time delay relative to the first electron. The multi-hit resolution, i.e., the minimum time delay between two electrons required to identify them as separate particles, was 10 ns. As a result of this deadtime, in the experiment only triple ionization events are recorded in which the longitudinal momentum between any two electrons differs at least by an amount Δp_1 given by the approximate relation $\Delta p_1 = 0.1\ \text{a.u.} + 0.07 * p_{11} * p_{12}$, where p_{11} and p_{12} are the longitudinal momentum components of the two involved electrons.

The electron detector was set in coincidence with both the recoil ion detector and the projectile detector. From the coincidence the time of flight of the recoil ions and the ionized electrons from the collision to the respective detector were obtained with a resolution of better than 1 nsec. From the time of flight, in turn, the momentum component in the longitudinal direction was determined. The two transverse components were deduced from the position information.

III. RESULTS AND DISCUSSION

A. Momentum balance between recoil ion and electron sum momentum

In Fig. 2 the momentum distributions in the plane defined by the initial projectile beam direction and the outgoing recoil ion momentum vector are shown for Ne^{3+} recoil ions and the sum momentum of the three ionized electrons. The horizontal and vertical axis represent the parallel (longitudinal) momentum component and the projection of the perpendicular (transverse) component onto the plane defined above. Two features in this spectrum should be pointed out: first, the recoil ion and electron sum momentum distributions are aligned in opposite directions. Second, there is an obvious forward-backward asymmetry in the longitudinal direction with the sum momentum vector of the electrons pointing in the forward direction and the recoil momentum vector pointing in the backward direction. Very similar characteristics were observed by Moshhammer, *et al.* [18] and theoretically reproduced by Olson *et al.* [19] for single ionization of He by 3.6 MeV/amu Se^{28+} impact. They pointed out that the opposite direction of the recoil ion and the electron momenta

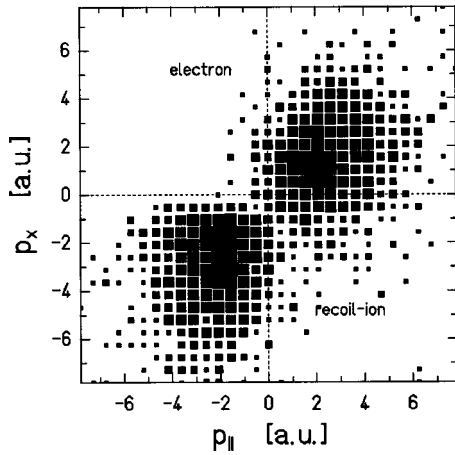


FIG. 2. Distribution of the sum momentum vector of the three ionized electrons (upper part) and of the recoil ions (lower part). The horizontal axis is the longitudinal and the vertical axis the projection of the transverse momentum component onto the collision plane.

reveals a close connection between ionization by energetic heavy ion impact and photoionization. Since the momentum transfer in a photoionization event is negligible, the recoiling target ion has to compensate the sum-momentum of all emitted electrons. Therefore, the recoil ion and electron momentum vectors must point in opposite directions or, to turn the conclusion around, the fact that they do proves that the momentum transfer from the projectile is small.

The small momentum transfer, i.e., the momentum change of the projectile, in the longitudinal direction can simply be explained by kinematics. For small projectile scattering angles, which is always well fulfilled for energetic heavy ion impact (for our collision system the scattering angles are essentially never larger than $1 \mu\text{rad}$), it can be shown that the longitudinal momentum transfer is given by the projectile energy loss ΔE divided by the initial projectile velocity v_0 . For triple ionization in this collision system, the energy loss distribution maximizes around 250 eV [17]. With a projectile velocity of 12 a.u. this yields a longitudinal momentum transfer of 0.75 a.u., which is small compared to the width of the electron and recoil ion momentum distributions.

The small momentum transfer in the transverse direction, in contrast, is not just a kinematic effect, rather it provides some information about the mechanism leading to triple ionization. For example, binary collisions between the projectile and the electrons can be ruled out as an important contributor. There, the recoil ion would be a passive spectator and would gain a relatively small momentum without any favored direction relative to the electrons. At the same time from the projectile energy dependence of total double ionization cross sections it is known that independent interactions of the projectile with each electron is the dominant mechanism for the perturbation regime studied here ($Q/v_0=4.4$) [20–22]. It is reasonable to assume that this is also true for a higher degree of ionization. Therefore, the close relation between ionization by charged particle impact and photoionization pointed out by Moshhammer *et al.* for single ionization [18] is observed here for triple ionization as well. In a simple

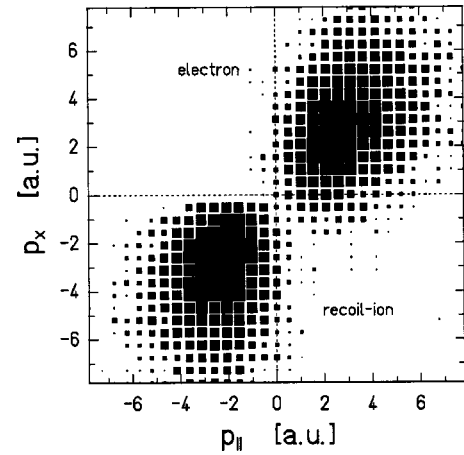


FIG. 3. Distribution of the sum momentum vector of the three ionized electrons (upper part) and of the recoil ions (lower part) calculated with the nCTMC model. The axis have the same meaning as in Fig. 2.

picture, the projectiles serve as a provider of virtual photons, through which energy, but not much momentum can be transferred [23,24].

For photoionization, one would expect the momentum distribution of the recoil ions and electrons to be oriented along the transverse direction (electric dipole distribution). The fact that in the experiment these distributions are rotated toward the longitudinal direction was conclusively interpreted as due to the postcollision interaction (PCI) in the case of single ionization [18,19]. The projectile is “pulling” the electrons along in the forward direction and “pushing” the recoil ions in the backward direction. In our data the forward focusing of the electrons is more pronounced than in these references illustrating that the total effect of the PCI is even more important for multiple ionization since each of the electrons is affected by it. Furthermore, for the collision system studied here the perturbation is larger than in the work of Moshhammer *et al.*

These features observed in the data are also very well reproduced by an nCTMC calculation [25], which is shown in Fig. 3. It is the only theory currently available for multiple ionization which properly accounts for the interactions of the target nucleus and the projectile with all ionized electrons throughout the entire collision. In particular, this also means that the PCI is fully included. As a result, the photoionization characteristics and the forward-backward asymmetry observed in the experimental electron and recoil ion momentum distributions, which is generated by the PCI, are also seen in the calculation.

B. Energy partitioning between the ionized electrons, Dalitz plots

Two major problems occur when potential correlations between three ionized electrons are to be explored: first, the strong PCI, although being an interesting research object in its own right which has been investigated in many different studies [18,26–31], might overshadow all mutual interactions between the electrons. The second problem is simply a

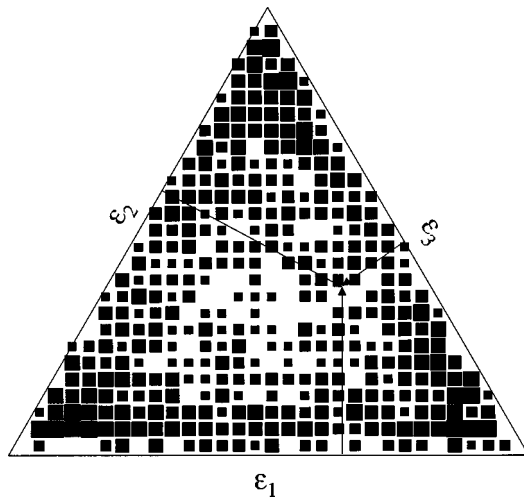


FIG. 4. Dalitz plot of the ionized electrons in the lab frame. The electrons are treated as equivalent particles, i.e., they are not labeled by any other quantity apart from their relative energy.

question of presenting the data. A signature of correlation would be if a certain quantity of one electron (e.g., its energy) was dependent on the corresponding quantity of the other two electrons. To see such an interdependence requires one to plot that quantity for all three electrons simultaneously in the same spectrum.

In particle physics, one method of representing the energies of three particles simultaneously in the same spectrum is known as Dalitz plot [32]. Recently, this kind of presentation was applied in atomic physics to study the fragmentation dynamics of the H_3^+ molecule [33]. In a Dalitz plot, the relative energy ε_i of each particle normalized to the sum energy of all three particles is plotted in a coordinate system consisting of an equilateral triangle. An example for the relative energies of three electrons is shown in Fig. 4 for our triple ionization data. For a given data point, the relative energy of each electron is given by the perpendicular distances of that data point to the three sides of the triangle, as indicated in Fig. 4 by the arrows. If the height of the triangle is normalized to unity, it can be shown by simple geometry that for any point inside the triangle the sum of all perpendicular distances to the three triangle sides is also 1. Therefore every data point is already unambiguously determined by two triangular coordinates (i.e., by the relative energies of two electrons).

Some structures are observable in Fig. 4. The data appear to accumulate near the triangle sides, especially near the triangle corners while there is a minimum near the center. However, in this plot a relatively small fraction of the information available from the data has been used. In particular, no information on the emission direction of the ionized electrons is provided. Furthermore, the ionized electrons are treated as equivalent particles in Fig. 4, i.e., they are not distinguished from each other by any quantity apart from their relative energies which are plotted. The structures observed in the Dalitz plots may become more pronounced by distinguishing the electrons in terms of additional measured quantities like, for example, the emission angle relative to

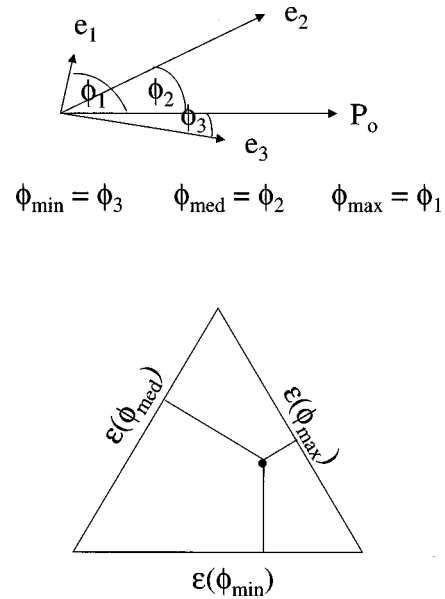


FIG. 5. Illustration of the distinction of the electrons by their emission angle. The top part shows as an example of a triple ionization event the momentum vectors of the electrons (arrows labeled e_1 , e_2 , and e_3) and the projectile direction (arrow labeled p_0) along with the electron emission angles relative to the projectile. The bottom part shows schematically how this event is presented in a Dalitz plot with the triangle sides being determined by the electron emission angle (see text).

the projectile direction and, more importantly, a larger amount of information is contained in a single spectrum.

The exact definition of the electron emission angles and the distinction of the electrons by that angle is illustrated in Fig. 5. In the top part, it shows an example of a triple ionization event with the momentum vectors of the three electrons (arrows labeled as e_1 , e_2 , and e_3) and the initial projectile direction (arrow labeled as p_0). The emission angle for each electron is defined as the angle between its momentum vector and the projectile direction vector such that it takes values between 0° and 180° . We can now proceed to distinguish the electrons by their emission angles in the Dalitz plots. In our example the angle of electron 3 is the smallest of the three angles and the one of electron 1 is the largest. For each triple ionization it can be determined which electron has the minimal, medium, and maximal emission angle in this way. In a Dalitz plot the relative energy of the electron with the minimal angle can now be plotted as the perpendicular distance to one specific triangle side, say the lower side. Likewise, the relative energies of the electrons with the medium and maximal angles are represented by the left and right triangle sides, respectively. This is illustrated for our example in the bottom part of Fig. 5. Electron 2 has the largest energy and the medium emission angle and electron 1 has the smallest energy and the maximal angle. Therefore, this particular event has to be presented in the Dalitz plot by a data point which is closest to the right and furthest from the left triangle side.

In Fig. 6 a Dalitz plot with the electrons labeled by their emission angles is shown. This labeling of the electrons in-

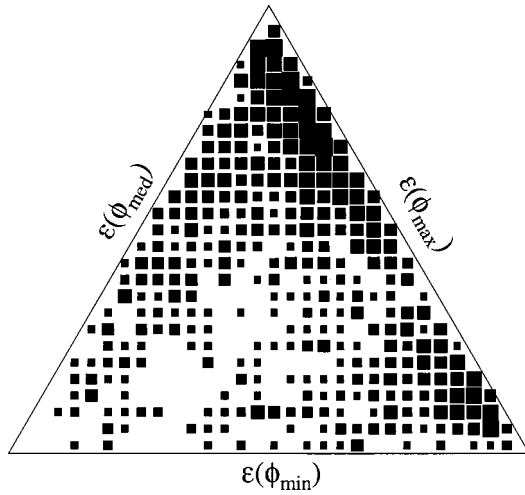


FIG. 6. Dalitz plot with the electrons being labeled by their emission angle relative to the projectile direction according to the scheme illustrated in Fig. 5.

deed leads to an enhancement of the structure which is apparent already in Fig. 4 and additional information about the collision dynamics can be extracted from the data. Now this structure, which in Fig. 4 occurs near all triangle sides, is compressed to a region close to only one triangle side, the one corresponding to the electron with the largest emission angle. In fact, the main contribution occurs near the top corner of the triangle. This means that very asymmetric energy distributions with one fast and two slow electrons are strongly favored. The electron with the smallest emission angle is most likely the fastest electron. A second, although much weaker maximum is observable near the lower right corner of the triangle corresponding to events where the electron with the medium emission angle is fast and the other two electrons remain almost at rest. The observed structure means that the continuum reveals a surprisingly high degree of order rather than a chaotic behavior which would be reflected by a more uniform energy distribution with similar contributions from symmetric and very asymmetric partitions.

One should be cautious not to prematurely interpret the pronounced structure in the data as due to electron correlation effects. In particular the importance of the PCI for the collision system studied here should be kept in mind. It cannot be ruled out that the PCI leads to peak structures in the Dalitz plot for triple ionization. In order to conclusively explain the features in the data it is important to compare to theoretical models which fully include the PCI. Ideally, these calculations should be performed with and without the electron-electron interaction included throughout the collision. The experimental observations which have to be reproduced by theory can be summarized in two points: (1) the three-electron continuum is strongly structured favoring very asymmetric energy distributions with one fast and two slow electrons indicating some degree of order. (2) There is a pronounced correlation between the emission angle and the relative energy of the electrons in that the fast electron is almost exclusively the one with the smallest emission angle.

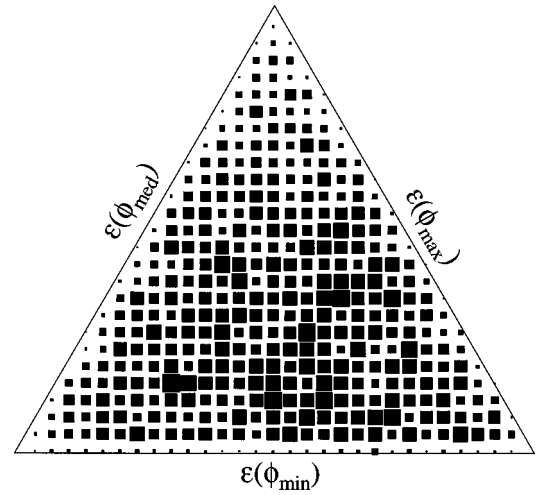


FIG. 7. Dalitz plot calculated with the nCTMC model. The electrons are labeled the same way as for the data in Fig. 6.

Theoretical models for triple ionization with the electron-electron interaction fully included are currently not available. We therefore first discuss the data in comparison with the nCTMC method which considers the ionized electrons to be independent of each other. In the next section we will then attempt a qualitative analysis by modeling the electron-electron interaction in a rather simplified manner. In Fig. 7 a Dalitz plot calculated with the nCTMC model with the electrons labeled the same way as in Fig. 6 is shown. This model has been successfully applied to calculate important quantities like the recoil ion charge state distribution [34], electron energy and angular differential cross sections [35], recoil-ion momentum distributions [34] and, recently, the projectile energy-loss spectra in multiple ionization [17]. Moreover, it describes well the momentum balance between the recoil ion and the electron sum momentum vector (see above). However, the electron-electron interaction is only incorporated in so far as the total binding energy of all electrons in the atom is reproduced correctly by using appropriate electron screening functions in the initial state.

The nCTMC model yields a fairly uniform energy distribution without a pronounced structure, as expected for a calculation without electron correlations. In particular, near the top corner of the triangle, where the data show the most pronounced structure, there is essentially no intensity in this calculation. However, the calculation presented in Fig. 7 has not been convoluted to the experimental restrictions of electron transverse momenta of less than 3.5 a.u. and those imposed by the multi-hit deadtime (see experimental section). In Fig. 8 we show the nCTMC calculation corrected for these experimental restrictions. The major difference to the calculation without the correction is a line of reduced intensity approximately extending from the lower left corner to the midpoint of the right side of the triangle. This is mainly an effect of the multihit deadtime. Otherwise, the basic shape of the Dalitz plot in Fig. 7 is maintained in Fig. 8, most importantly there is still essentially no intensity in the triangle corners.

As mentioned above the nCTMC model has been very successful in describing quantities in multiple ionization

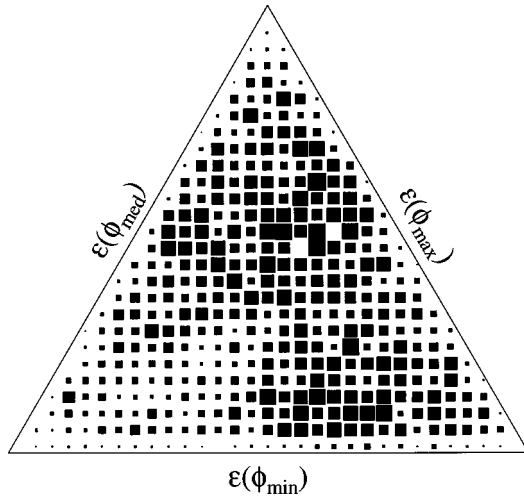


FIG. 8. Same as Fig. 7 with the calculation corrected for the experimental restrictions in the electron momentum distributions (see text).

which are not sensitive to the electron-electron interaction. Moreover it is known to correctly account for the PCI [18,19]. We can therefore safely rule out the PCI as the sole contributor to the structure observed in the data. Rather, the comparison between the data and the calculation suggests that these structures are in some way related to the electron-electron interaction. Furthermore, the fairly uniform distribution indicates that the ten-body nCTMC model does not lead to a high degree of order in the many-electron continuum.

C. Qualitative analysis of the role of the electron-electron interaction

Since no theoretical method is currently available for triple ionization which includes the electron-electron interaction throughout the entire collision, in this section we attempt to qualitatively interpret the structures observed in the data by modeling the electron-electron interaction in a simplified manner. Specifically, we will address the question whether potential electron correlations are particularly important in the initial or in the final state or whether a combination of both is required to explain the data. This also relates to the question spelled out in the introduction concerning the ordered structure (or lack thereof) of several electrons ionized in a collision. If, for example, the structures in the data could be explained only by incorporating initial state electron correlations this would indicate that in a triple ionization event the ordered structure of the initial state is mapped onto the continuum state. Likewise, a dominance of a final state correlation could be interpreted as the electron-electron interaction in the continuum generating a new order unrelated to the initial state. We would like to stress, however, that our models described below should not be viewed primarily as a theoretical effort to explain the data quantitatively, but rather as a means to analyze the data qualitatively. We realize that full theoretical calculations incorporating the electron-electron interaction in a more sophisticated manner are needed and we hope that our work will initiate such theoretical efforts.

The nCTMC code serves as the theoretical foundation for our modeling efforts, where the role of the electron-electron interaction was analyzed by applying two different methods. In the first model, an electron-electron correlation in the initial target state is simulated. Here a five-body collision with 3 electrons in the $2p$ state is assumed. The electrons initially orbit the nucleus on 3 elliptical trajectories in the same plane with the major axis making an angle of 120° relative to each other. The initial condition is chosen such that the electrons are synchronized to the same distance from the nucleus at all times in orbits of equal eccentricity. This imitates the repulsive electron-electron force in the initial state by keeping the electrons as far apart from one another as possible. However, the electron-electron interaction is not incorporated in the evolution of the system during the collision. In the following we refer to this model as CTMC-IC (IC stands for initial state correlation).

In the second model the initial state is chosen in the same manner as in the CTMC-IC model. However, now the electron-electron interaction between all three electrons is fully included throughout the collision, i.e., electron-electron correlations in the final continuum state are included as well. This model we call CTMC-FC (FC stands for full correlation).

The results of these CTMC models are shown in Fig. 9 (center: CTMC-IC, bottom: CTMC-FC). For comparison, in the top we show again the original nCTMC calculation without the electron-electron interaction. The CTMC-IC model qualitatively reproduces one major feature observed in the data: it also shows peak structures near the upper and lower right triangle corners, i.e., it predicts that a very asymmetric energy distribution with one fast and two slow electrons is strongly favored. However, in the calculation the intensities of these two peaks are reversed compared to the data. In the CTMC-IC model the electron with the medium rather than the minimal emission angle is most likely the fast electron. Finally, the CTMC-FC model provides a very good qualitative description of the data. It not only reproduces the asymmetric energy distribution among the three electrons, as the CTMC-IC does, but it also predicts correctly that the electron with the smallest emission angle is the fast electron. The models of Fig. 9 are shown without the corrections for the restrictions in the measured momentum distributions in order to illustrate the effects of the electron-electron interaction independently of any experimental condition. In the CTMC-FC model this correction has the same influence as in the nCTMC calculation in that it leads to a reduced intensity along a line extending from the lower left corner to the midpoint of the right side of the triangle. This leads to an improved agreement with the data.

The comparison between the data and the various CTMC models suggests that electron-electron correlations both in the initial state and in the final continuum state are important. The initial state correlation seems to be the decisive factor in determining the energy partitioning. Without labeling the electrons by their emission angle the CTMC-IC model, i.e., a model which does not incorporate any final state correlation, provides already an adequate picture (Fig. 4 is qualitatively well described by this model). The final state correlation, in

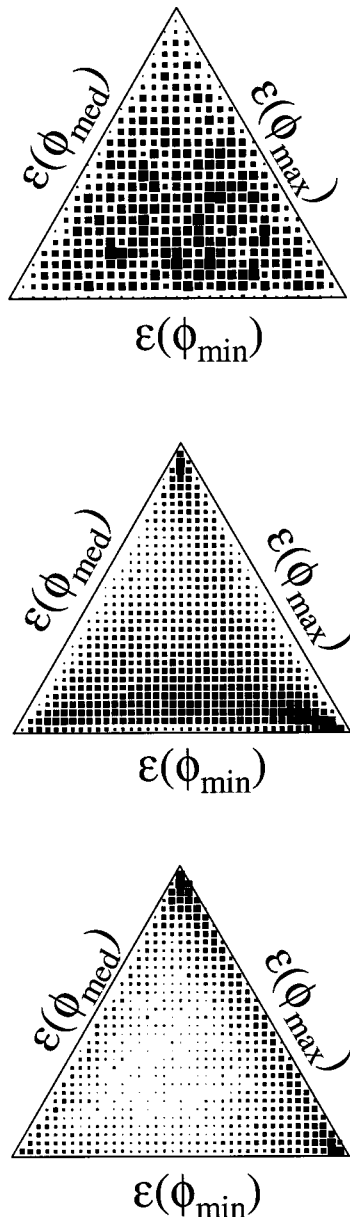


FIG. 9. Calculated Dalitz plots using various CTMC models: nCTMC (same as Fig. 7, top), with simulation of electron correlations only in the initial state (CTMC-IC center), and same as CTMC-IC, but with electron-electron interaction in the final continuum state included (CTMC-FC, bottom).

contrast, predominantly affects the angular distribution of the electrons since without it the CTMC model does not predict correctly the relation between emission angle and relative energy. This comparison between the CTMC-IC and CTMC-FC models also indicates that the high degree of order in the three-electron continuum reflected by the sharp peak structures contains two components: first, to some extent the initial order of the stationary target atom is apparently imaged into the continuum leading to the asymmetric energy distribution. Second, the electron-electron interaction in the continuum appears to generate an additional new order unrelated to the initial state leading to a connection between the emission angle and the relative energy of the ionized

electrons.

While the CTMC-FC model is in good qualitative agreement with the data, quantitatively there are some discrepancies. The structures in the calculation are more pronounced and more focused around the upper triangle corner than in the data. Such quantitative discrepancies are not surprising since the electron-electron correlations, especially in the initial state, are certainly modeled in a simplified manner. In particular, the initial state correlation is overestimated by keeping the electrons as far apart from each other as possible. While one would expect that the mutual repulsion leads to a somewhat increased distance, it is, of course, unrealistic to assume that the electrons maintain at all times a maximum distance. However, the advantage of this model is that the final state dynamics are correctly portrayed by the five-body pairwise Coulomb interactions.

IV. CONCLUSIONS

In this paper we have presented a kinematically complete experiment on triple ionization. We have demonstrated that Dalitz plots are a very efficient method to simultaneously present the energies of three particles in a single spectrum. This is crucially important in order to analyze the interrelation between the three involved particles. Plotting the energy of only two particles, for example, is equivalent to integrating of the third particle and valuable information on possible correlation effects may be lost.

Our data show that in triple ionization highly asymmetric energy distributions with one fast and two slow electrons are strongly favored. The fast electron is almost always the one with the smallest emission angle relative to the projectile direction. This behavior cannot be reproduced by our nCTMC calculation, which does not include the electron-electron interaction. However, if the electron-electron interaction is incorporated throughout the collision, although in a greatly simplified manner, very good qualitative agreement is achieved. The comparison between the data and theory suggests that the very asymmetric energy distribution is generated by an electron-electron correlation in the initial target state, while the predominantly small emission angles for the fast electrons are caused by the electron-electron interaction in the final continuum state. We are therefore led to conclude that a proper incorporation of the electron-electron interaction is critical in both the initial and the final state. This supports the conclusion of Bapat *et al.* [16] that it is not possible to separate the electron-electron interaction in the initial from the one in the final state.

ACKNOWLEDGMENTS

One of us (M.S.) is grateful for the hospitality of the Gesellschaft für Schwerionenforschung and the University of Freiburg. This work was supported by Gesellschaft für Schwerionenforschung, the Leibniz-Programm and the SFB276 Projekt B8 of the Deutsche Forschungsgemeinschaft, the National Science Foundation, and the Office of Fusion Energy Sciences and the Division of Chemical Sciences of the Department of Energy.

- [1] J. Ullrich, R. Moshhammer, R. Dörner, O. Jagutzki, V. Mergel, H. Schmidt-Böcking, and L. Spielberger, *J. Phys. B* **30**, 2917 (1997), and references therein.
- [2] L. Gulyas, P. D. Fainstein, and A. Salin, *J. Phys. B* **28**, 245 (1995).
- [3] M. McCartney and D. S. F. Crothers, *J. Phys. B* **26**, 4561 (1993).
- [4] J. H. McGuire, *Adv. At., Mol., Opt. Phys.* **29**, 217 (1992), and references therein.
- [5] J. F. Reading and A. L. Ford, *Phys. Rev. Lett.* **58**, 543 (1987).
- [6] J. H. McGuire, *J. Phys. B* **28**, 913 (1995).
- [7] S. Keller, H. J. Lüdde, and R. M. Dreizler, *Phys. Rev. A* **55**, 4215 (1997).
- [8] C. J. Wood, R. E. Olson, W. Schmidt, R. Moshhammer, and J. Ullrich, *Phys. Rev. A* **56**, 3746 (1997).
- [9] H. J. Lüdde, A. Henne, T. Kirchner, and R. M. Dreizler, *J. Phys. B* **29**, 4423 (1996).
- [10] I. E. McCarthy and E. Weigold, *Rep. Prog. Phys.* **54**, 789 (1991), and references therein.
- [11] J. Berakdar, *Phys. Rev. A* **53**, 2314 (1996).
- [12] R. Moshhammer, J. Ullrich, M. Unverzagt, W. Schmitt, P. Jardin, R. E. Olson, R. Mann, R. Dörner, V. Mergel, U. Buck, and H. Schmidt-Böcking, *Phys. Rev. Lett.* **73**, 3371 (1994).
- [13] R. Moshhammer, J. Ullrich, H. Kollmus, W. Schmitt, M. Unverzagt, O. Jagutzki, V. Mergel, H. Schmidt-Böcking, R. Mann, C. J. Woods, and R. E. Olson, *Phys. Rev. Lett.* **77**, 1242 (1996).
- [14] I. Iaouil, A. Lahmam-Bennani, A. Duguet, and L. Avaldi, *Phys. Rev. Lett.* **81**, 4600 (1998).
- [15] A. Dorn, R. Moshhammer, C. D. Schröter, T. J. M. Zouros, W. Schmitt, H. Kollmus, R. Mann, and J. Ullrich, *Phys. Rev. Lett.* **82**, 2496 (1999).
- [16] B. Bapat, R. Moshhammer, S. Keller, W. Schmitt, A. Cassimi, L. Adoui, H. Kollmus, R. Dörner, T. Weber, K. Khayat, R. Mann, J. P. Grandin, and J. Ullrich, *J. Phys. B* **32**, 1859 (1999).
- [17] M. Schulz, R. Moshhammer, W. Schmitt, H. Kollmus, R. Mann, S. Hagmann, R. E. Olson, and J. Ullrich, *J. Phys. B* **32**, L557 (1999).
- [18] R. Moshhammer, J. Ullrich, H. Kollmus, W. Schmitt, M. Unverzagt, H. Schmidt-Böcking, C. J. Wood, and R. E. Olson, *Phys. Rev. A* **56**, 1351 (1997).
- [19] R. E. Olson, C. J. Wood, H. Schmidt-Böcking, R. Moshhammer, and J. Ullrich, *Phys. Rev. A* **58**, 270 (1998).
- [20] J. H. McGuire, A. Müller, B. Schuch, W. Groh, and E. Salzborn, *Phys. Rev. A* **35**, 2479 (1987).
- [21] H. Knudsen, L. H. Andersen, P. Hvelplund, G. Astner, H. Cedergquist, H. Danared, and L. Liljeby, *J. Phys. B* **17**, 3545 (1984).
- [22] J. Ullrich, R. Moshhammer, H. Berg, R. Mann, H. Tawara, R. Dörner, J. Euler, H. Schmidt-Böcking, S. Hagmann, C. L. Cocke, M. Unverzagt, S. Lencinas, and V. Mergel, *Phys. Rev. Lett.* **71**, 1697 (1993).
- [23] C. F. Weizsäcker, *Z. Phys.* **88**, 612 (1934).
- [24] E. J. Williams, *Phys. Rev.* **45**, 729 (1934).
- [25] R. E. Olson, J. Ullrich, and H. Schmidt-Böcking, *Phys. Rev. A* **39**, 5572 (1989).
- [26] G. B. Crooks and M. E. Rudd, *Phys. Rev. Lett.* **25**, 1599 (1970).
- [27] K. G. Harrison and M. W. Lucas, *Phys. Lett.* **33A**, 142 (1970).
- [28] W. Meckbach, I. B. Nemirovsky, and C. R. Garibotti, *Phys. Rev. A* **24**, 1793 (1981).
- [29] O. Jagutzki, R. Koch, A. Skutlarz, C. Kelbch, and H. Schmidt-Böcking, *J. Phys. B* **24**, 993 (1991).
- [30] T. Vajnai, A. D. Gaus, J. A. Brand, W. Htwe, D. H. Madison, R. E. Olson, J. L. Peacher, and M. Schulz, *Phys. Rev. Lett.* **74**, 3588 (1995).
- [31] M. Schulz, T. Vajnai, A. D. Gaus, W. Htwe, D. H. Madison, and R. E. Olson, *Phys. Rev. A* **54**, 2951 (1996).
- [32] R. H. Dalitz, *Philos. Mag.* **44**, 1068 (1953).
- [33] L. M. Wiese, O. Yenen, B. Thaden, and D. H. Jaecks, *Phys. Rev. Lett.* **79**, 4982 (1997).
- [34] M. Unverzagt, R. Moshhammer, W. Schmitt, R. E. Olson, P. Jardin, V. Mergel, J. Ullrich, and H. Schmidt-Böcking, *Phys. Rev. Lett.* **76**, 1043 (1996).
- [35] W. Wolff, H. E. Wolff, J. L. Shinpaugh, J. Wang, R. E. Olson, P. D. Fainstein, S. Lencinas, U. Bechthold, R. Herrmann, and H. Schmidt-Böcking, *J. Phys. B* **26**, 4169 (1993).